2025 IEEE/SICE International Symposium on System Integration (SII)
January 21-24, 2025, Munich, Germany

Time Series Prediction of Sit-to-Stand Muscle Synergy Using Deep Learning

Julian Ilham[1] Yuichi Nakamura[1] Takahide Ito[2] Kazuaki Kondo[1] Jun-ichiro Furukawa[2]
Qi An[3] Kei Shimonishi[1]

***Abstract*— Sit-to-stand (STS) motion is a complex behavior and requires a high power, especially when included in activities of daily living. For people with difficulties in performing this motion, assistive devices are particularly suitable. Although assistive devices should timely activate for providing assistance, they often exhibit multiple inherent delays. We introduce a control scheme intended to ensure proper timing for triggering assistive devices by predicting user's STS motion intention. We employ electromyography and muscle synergy and design a deep neural network to predict motion intention. The proposed network is evaluated in terms of the accuracy and anticipation time of the predicted motion according to the forecast time considered during network training. The accuracy decreases with increasing forecast time. In addition, a longer forecast time for training increases the inferred anticipation time. Our results suggest that the control of assistive devices with proper timing and output power is feasible by implementing the proposed control scheme.**

I. INTRODUCTION

Sit-to-stand (STS) motion is a complex behavior and one of the most power-demanding tasks to perform activities of daily living. Hence, assistive devices are required for people who have difficulties in performing STS motion. We aim to develop a control scheme for such assistive devices, currently focusing on device activation at the proper timing by detecting user's STS intention. We consider two assistive devices: 1) assistive chair and 2) exoskeleton for the knee joint [1], [2], [3]. The chair mainly assists the user in lifting the trunk while keeping the center of mass within the base of support. The exoskeleton assists the user's knee extension by delivering adequate torques. The devices can work either independently or collaboratively.

Assistive devices should start operation when the user intends to perform an STS motion. Timely activation is essential to avoid accidents, such as falls, and elicit the user's feeling of self-agency. In addition, we need to consider that assistive devices require a period, t_A, for activation. For example, approximately 100 ms are required for pneumatic artificial muscles to deliver their full strength. Hence, assistive devices should be triggered before user's motion begins. This type of delay can be handled by predicting user's motion. Moreover, it is desirable that the anticipation time for prediction is longer than the total latency, t_L, which is the sum of the measurement latency, time for computation and communication, and time for assistive device activation.

*This work was supported by JSPS, Japan KAKENHI Grant No.: JP21H04894

[1]Julian Ilham, Yuichi Nakamura, Kazuaki Kondo, and Kei Shimonishi are with the Academic Center for Computing and Media Studies, Kyoto University, Kyoto, Japan {jilham@ccm., yuichi@}media.kyoto-u.ac.jp

[2]Takahide Ito and Jun-ichiro Furukawa are with Man-Machine Collaboration Research Team, Guardian Robot Project, RIKEN, Kyoto, Japan

[3]Qi An is with the Graduate School of Frontier Sciences, The University of Tokyo, Chiba, Japan

II. BACKGROUND

Initial posture changes are often used as cues of motion intention [4], [5], [6]. However, such cues lead to serious delays because posture changes result from muscle contraction that takes certain time. Unlike cyclic motions such as walking, STS motion is non-cyclic and generally executed while sitting on a chair, bed, floor, etc. Consequently, it does not exhibit a typical preceding motion or repetitive cycle that can be used for reliable time series prediction.

To handle this limitation, we perform motion prediction based on electromyography (EMG) signals, which precede actual muscle contraction by 30–100 ms [7] for estimation with a suitable anticipation. Various problems appear when using EMG. One problem is fluctuations. The activity of a single muscle captured as an EMG signal shows non-negligible fluctuations, and it may fail to constitute a stable cue for motion intention. For example, reaching for an object in front of a user causes muscle activation resembling that of the first phase of STS motion of leaning the trunk forward. Another problem is the insufficient anticipation time. The anticipation time that can be achieved from an EMG signal is still shorter than activation latency, t_L, required for a typical assistive device. Consequently, using EMG alone is insufficient for timely activation of assitive devices. Alternatively, we perform motion prediction considering muscle synergy, which involves neuromuscular coordination for recruiting various muscles to perform specific motions. The activation of muscle synergy is less affected by fluctuations of individual muscle activity because recruited muscles cooperate to perform the target motion. Moreover, every muscle synergy pattern closely reflects specific movements around a joint [8]. The amount of muscle synergy activation is related to the corresponding joint torque, possibly providing valuable information for controlling assistive devices. For predicting muscle synergy, we adopt time series prediction using a deep neural network (DNN). As a result, assistive devices can start proper operations before actual torque (force) is needed to be delivered when the anticipation time for prediction is longer than the total activation latency, t_L.

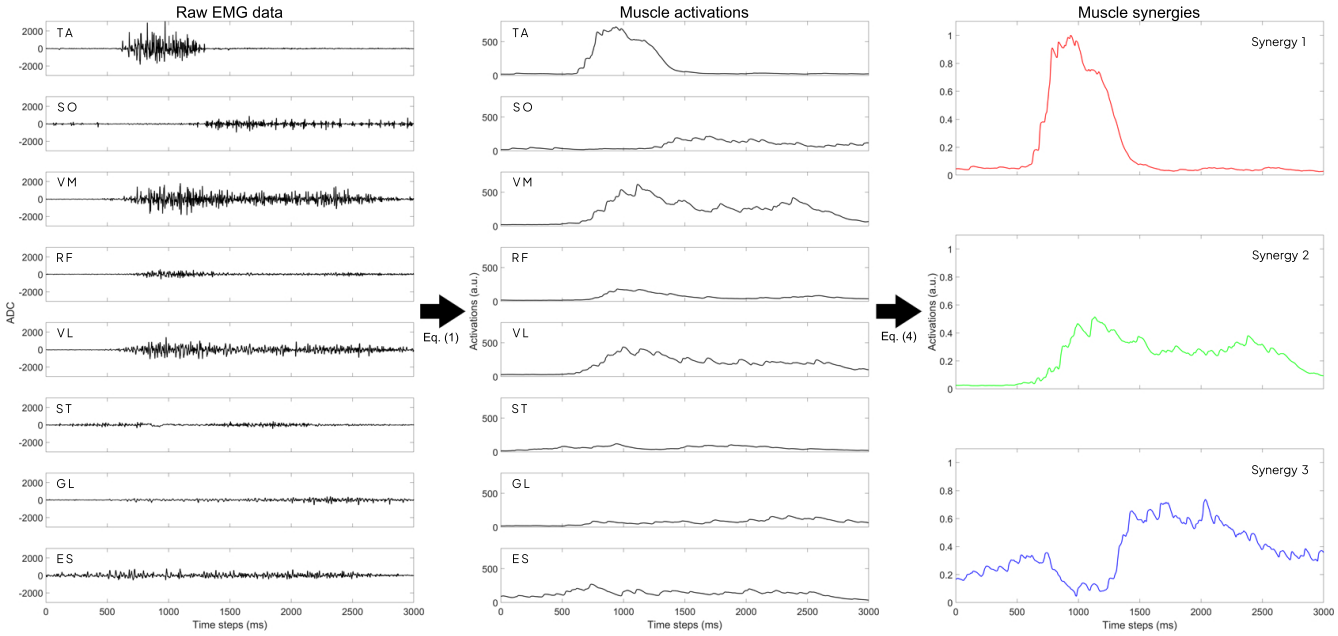

Fig. 1: Example of raw EMG data ($\boldsymbol{u}$), muscle activation (A_s), and muscle synergy (H_s) of a single STS motion.

III. MUSCLE ACTIVITY MEASUREMENT

We measured EMG signals from eight outer muscles that contribute to STS motion: tibialis anterior (TA), soleus (SO), vastus medialis (VM), rectus femoris (RF), vastus lateralis (VL), semitendinosus (ST), gluteus medius (GL), and erector spinae (ES). Measured electric potential differences were amplified by a factor of 1000, high-pass filtered at a cutoff frequency of 10 Hz, and digitized at 1 kHz with 14 bits. Muscle activation m was calculated from the obtained EMG signal as proposed in [9]:

$$\begin{aligned} \dot{e} &= \frac{u-e}{\tau_{ne}} \\ \dot{m} &= \frac{e-m}{\tau} \\ \tau &= \begin{cases} \tau_{ac}, & \text{if } e \geq m \\ \tau_{deac}, & \text{if } e < m \end{cases} \end{aligned} \tag{1}$$

where e indicates the intermediate variable (i.e., muscle excitation), u represents the raw EMG signal, and τ_{ne}, τ_{ac}, and τ_{deac} are the time constants for muscle excitation, activation, and deactivation, respectively. These parameters were set as proposed in [9].

The observed signals expressed as

$$\begin{aligned} \boldsymbol{m}_i &= [m_i(t_{\text{begin}}), \ldots, m_i(t_{\text{end}})] \\ A &= [\boldsymbol{m}_1, \ldots, \boldsymbol{m}_n]^T \end{aligned} \tag{2}$$

where $\boldsymbol{m}_i$ represents the muscle activation sequence of i-th muscle, n is the number of muscles, and A represents the muscle activations of the measured muscles.

Then, muscle synergy patterns are calculated by applying concatenated non-negative matrix factorization (CNMF) [10], [11], [12]:

$$\begin{aligned} A_C &= [A_1, A_2, \ldots, A_k] \\ A_C &= WH + Err \\ W &= [\boldsymbol{w}_1, \boldsymbol{w}_2, \cdots, \boldsymbol{w}_N] \\ H &= [\boldsymbol{h}_1, \boldsymbol{h}_2, \cdots, \boldsymbol{h}_N]^T \end{aligned} \tag{3}$$

where A_C is the concatenation of A_is with k trials, A_i represents the muscle activation at trial i, N is the number of muscle synergy, W represents spatial patterns of muscle synergy, each of which is a column vector $\boldsymbol{w}_i$ comprising a set of time-invariant muscle contribution levels, H represents temporal patterns, each of which is a row vector $\boldsymbol{h}_i$ containing the time-varying activation of the corresponding spatial patterns, and Err is the residual of CNMF.

CNMF was used because applying NMF to concatenated data over multiple trials provides more stable muscle synergy patterns than conventional NMF of a single trial [11], [12]. We did not apply a low-pass filter, such as a Butterwoth 4 Hz low-pass filter used in previous studies, because it causes delay (phase shift) that hampers real-time processing. An example of the data processing is illustrated in Fig. 1.

If we directly follow the calculation in equation (3), it should be applied to the entire motion data after acquisition. For real-time processing, where motion data are acquired in a stream, we modified the formulation as follows:

$$H_s = A_s \backslash W_r \tag{4}$$

where A_s represents muscle activation data sequentially obtained in real time, W_r denotes the representative spatial pattern calculated for prerecorded samples, H_s represents the estimated temporal patterns, and operator $\backslash$ represents the least-squares solution that minimizes $W_r H_s - A_s$.

This approach assumes that muscle synergy does not change considerably in a short period, as considered in [12].

IV. PREDICTION OF MUSCLE SYNERGY

We designed a DNN to predict temporal patterns of muscle synergy.

A. DNN architecture

We designed a DNN structure with long short-term memory (LSTM) and fully connected (FC) layers. The inputs of the LSTM layer were temporal patterns of muscle synergy $H_s(t)$. The FC layer processed the outputs from the LSTM layer and predicted the values of temporal patterns a short time ahead.

B. DNN training and evaluation

For DNN training, EMG data for each participant were gathered. During training, the DNN learned to predict temporal patterns $H_s(t + t_F)$ from temporal patterns $H_s(t)$. A longer forecast time, t_F, was preferable to obtain sufficient anticipation time for device activation. However, longer t_F tended to degrade the prediction accuracy. Thus, we investigated the corresponding relationship. Multiple patterns of muscle synergy can occur, as shown by $\boldsymbol{w}_i$ and $\boldsymbol{h}_i$ in equation (3), and each pattern has a distinctive role in STS motion. Thus, we examined the prediction performance for each synergy pattern.

V. EXPERIMENTAL RESULTS

A. Data Acquisition

Five healthy male participants (age, 25.2 $\pm$ 5.4 years; weight, 66.2 $\pm$ 10.2 kg; height, 172.4 $\pm$ 2.9 cm) were recruited for this study. Each participant was asked to perform STS motions adopting the stabilization strategy [13], [14], [15]. This was because people who need power assistance usually adopt the safest STS strategy (i.e., stabilization strategy). The motion measurements were conducted in two sessions.

- S1: 20 trials of a single STS motion were performed with 1 minute intervals including rest between trials.
- S2: 15 trials of 3-minute-long motions including STS, stand-to-sit, and other natural motions while sitting were performed. Each trial contained from five to six STS motions.

From 75 to 90 samples of STS motions were collected per participant. EMG was measured for the above mentioned eight muscles via electrodes attached following the SENIAM guidelines [16]. A motion capture system and foot pressure sensor were used for recording and assisting in data segmentation and performance evaluation.

Each STS motion was segmented between 1000 ms before and 2000 ms after the seat-off event. The seat-off event onset was defined as the instant when the largest ground force for the backward direction measured by a force plate was observed while the hip left the chair. This event commonly occurs roughly in the first third of the total duration of STS motion [17].

Muscle synergy was calculated using the data collected from session S1. Note that, the extracted W in this calculation was also used as the representative spatial pattern W_r for real-time processing. Figure 2 shows an example of muscle synergy patterns. By obtaining three synergy patterns, the same as those considered in [12], the average VAF (variance accounted for) for all the trials was $89.36\% \pm 3.75\%$. This VAF was lower than that in previous studies, such as [12], mainly because linear low-pass filtering was not applied in our experiments, and small fluctuations in the signals affected the VAF [18], [19]. Thus, the VAF was close to the lower limit specified in [11].

The roles of the obtained synergy shown in Fig.2 can be explained as follows. Synergy 1 is dominated by muscles that regulate the ankle joint. Synergy 2 corresponds to the knee joint extension that produces the power required for standing up. Synergy 3 corresponds to the muscle activity to control the ankle, knee, and hip joints to balance the last phase of STS motion. These three types of synergies occur sequentially and with partial overlapping. Synergy 1 occurs first to control the leaning forward motion and move the center of mass into the base of support. Then, synergy 2 employs the leg power to lift the upper body. Finally, synergy 3 is gradually activated to balance the motion toward the final posture. The initial values of synergy 3 indicate certain muscle contraction while sitting still. However, the amount of contraction is not sufficient for detecting STS motion intention because it also appears when other motions are performed while sitting.

B. Performance Evaluation

The prediction performance was evaluated for data collected from session S2 with respect to five t_F values (4, 100, 200, 300, and 400 ms) as the forecast times. The data from session S2 were calculated using equation (4). The temporal patterns H_ss were divided to perform fivefold cross-validation. Each fold was split into 80% of samples for training, 10% for validation, and the remaining 10% for testing.

We evaluated the performance in terms of the accuracies and time shift (delay) of predicted values. Figure 3 shows two examples of temporal patterns and their predicted values in two ways. Solid lines indicate actual temporal patterns, H_s, and dashed lines indicate the predicted values, H_p. In the top row, predicted values $H_p(t)$ are mostly aligned with the original data. The figure shows similar trends for the predicted and original values, although some delay occurs for the prediction of synergy 1, while smaller delays appear for synergies 2 and 3. In the bottom row, predicted values $H_p(t - t_F)$ are aligned at the time that they are predicted, indicating the anticipation of prediction with respect to the actual (measured) values. Although most prediction results, especially for synergy 1, show certain delays as shown in the top row, the anticipation of predictions comes earlier than the actual signals, as shown in the lower row. Hence, suitable anticipation of actual motion occurs even for synergy 1, and it is better for synergies 2 and 3.

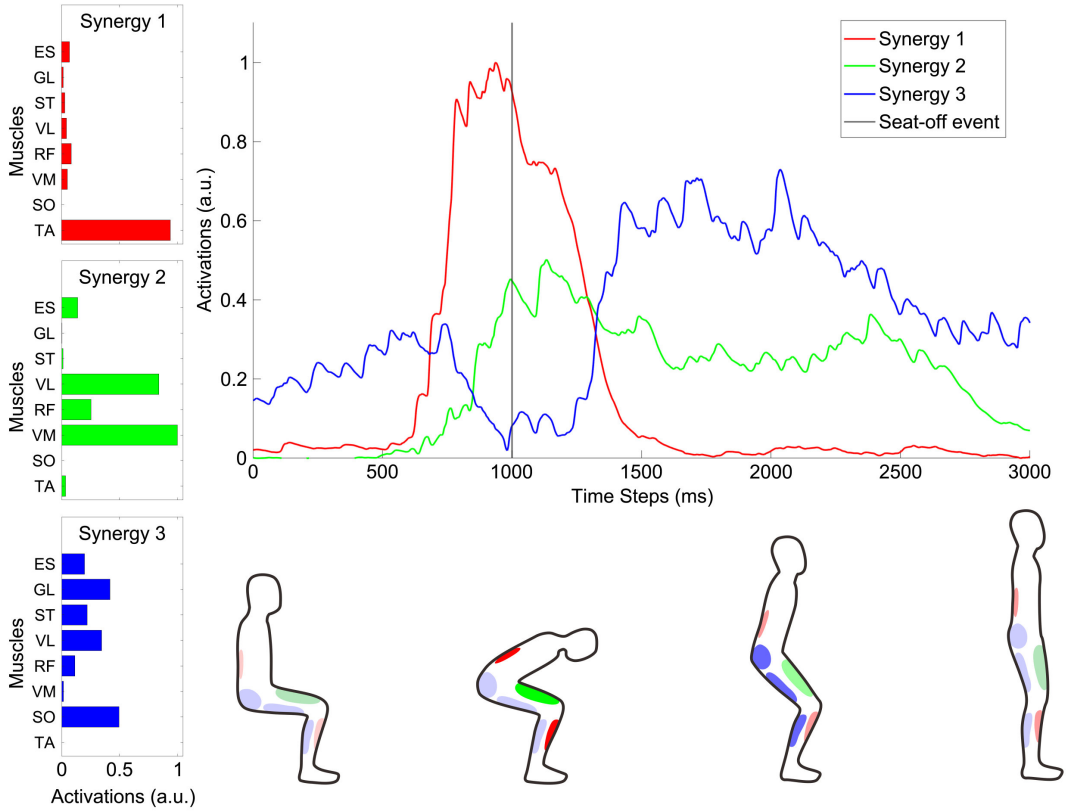

Fig. 2: Illustration of STS motion and examples of spatial patterns W (left column) and temporal patterns H (top-right graph).

The accuracy is evaluated as follows:

$$Accuracy_i = \left(1 - \frac{\sum_{t=1}^{t_{max}} \|\boldsymbol{h}_{i,p}(t) - \boldsymbol{h}_{i,s}(t)\|}{\sum_{t=1}^{t_{max}} \|\boldsymbol{h}_{i,s}(t)\|}\right) * 100\% \tag{5}$$

where $\boldsymbol{h}_{i,p}$ and $\boldsymbol{h}_{i,s}$ denote the predicted and original temporal patterns of i-th synergy, respectively.

Figure 4 shows the accuracy changes according to forecast time t_F. Similarity decreases with longer forecast time. The accuracy is slightly better for synergy 2 and worse for synergy 1.

To quantitatively examine the anticipation time, we define the center of the main slope as the point where the signal first rises up to 50% of the peak value as shown in Fig. 5. The time at the reference point is used for calculating the time difference between two signals. Let the reference time of the original signal be t_o, and that of the prediction be t_p. For each prediction condition, the anticipation time is given by t_o and t_p. Each prediction is obtained at time $t_p - t_F$, which implies $t_o - (t_p - t_F)$ is the anticipation time to the original signal denoted as t_{p-o}.

Figure 6 shows anticipation time t_{p-o} according to the forecast time, with major differences occuring among synergies 1–3. The anticipation time is smaller for synergy 1 and almost saturates with longer forecast time. Not enough preceding information is available at the beginning of synergy 1, thus hindering prediction. In contrast, a better anticipation time is obtained for synergies 2 and 3, for which the anticipation time becomes longer with increasing forecast time. Synergies 2 and 3 can be predicted by the preceding activation of muscles, such as those recruited for synergy 1.

VI. DISCUSSION

We examine the prediction performance of the proposed approach regarding the timing and amount of power assistance. We consider an automatic chair and knee exoskeleton as assistive devices. The chair should deliver force when the user begins to lift the hip from the seat, and the exoskeleton requires to deliver additional force when the user begins to extend the knee. Both actions occur simultaneously because knee extension causes the hip lift. Thus, the prediction of synergy 2 can contribute to natural and intuitive power assistance that delivers force at the beginning of knee extension. Hence, for a forecast time of 300 ms or higher, predicting the rapid increase in synergy 2 may provide sufficient information more than 200 ms before actual joint torque is necessary.

Synergies 1 and 3 have different roles, as mentioned in Section V-A. If an assistive device is intended to hold the ankle joint, we need to predict synergy 1. That would be more difficult than predicting synergy 2 because synergy 1 provides the weakest cues. The lack of preceding information before STS motion may be the main factor for these results. In contrast, synergy 3 is easier to predict using our scheme,

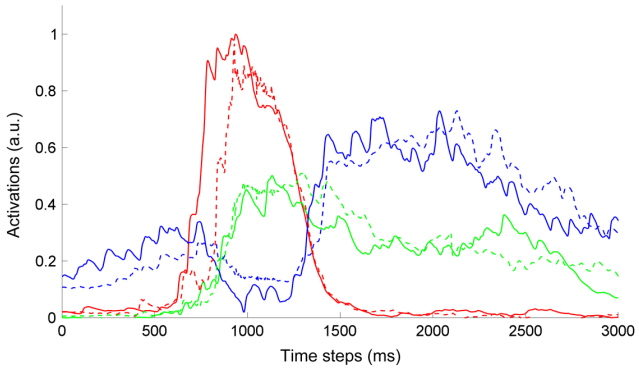

(a) $H_p(t)$ versus $H_s(t)$ of sample 1.

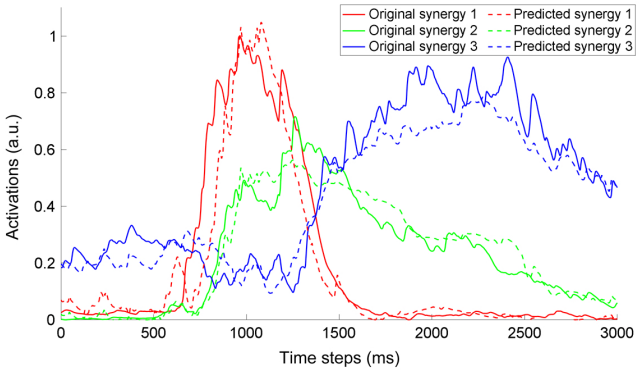

(b) $H_p(t)$ versus $H_s(t)$ of sample 2.

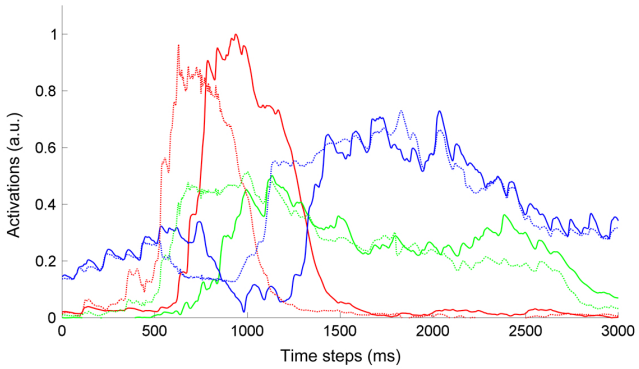

(c) $H_p(t - t_F)$ versus $H_s(t)$ of sample 1.

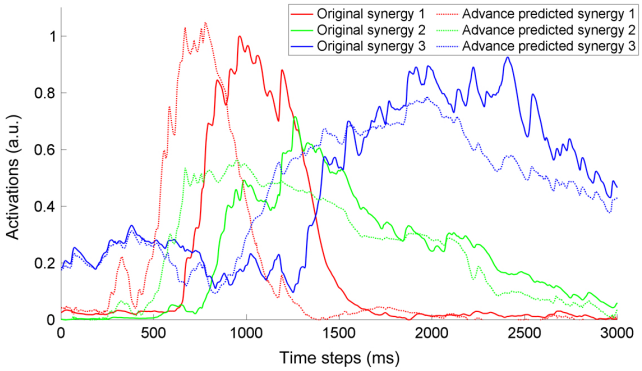

(d) $H_p(t - t_F)$ versus $H_s(t)$ of sample 2.

Fig. 3: Examples of temporal patterns and their prediction by DNN (forecast time t_F = 300 ms)

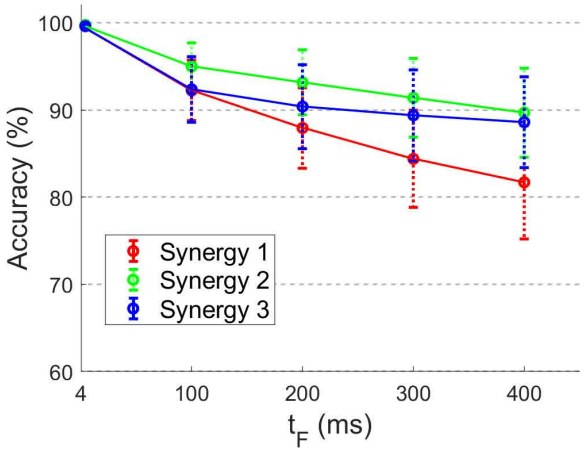

Fig. 4: Accuracy according to forecast time t_F.

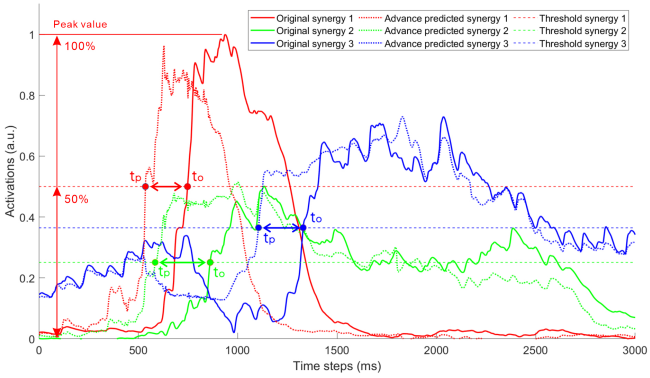

Fig. 5: Time difference t_{p-o} indicating anticipation time of actual muscle activation.

and we can expect timely assistance to maintain balance at the last phase of STS motion.

The activation of muscle synergy suggests the occurence of the corresponding joint torque. Hence, the required force/torque for assistance can be estimated by muscle synergy prediction. Our experimental results show the relationship between forecast time and accuracy, indicating an accuracy higher than 90% with 300 ms or lower forecast time for synergy 2. This gives a perspective on the accuracy for device control using prediction of STS motion. Conversely, verification with actual devices was beyond the scope of this study, because it involves specific device operation and users' behaviors. Such verification will be the subject of future work.

Only male participants were involved in this study, and the number of them is limited. Hence, the results cannot represent the general cases of population. More extensive work to include a larger number of participants and women should be done to achieve general conclusion.

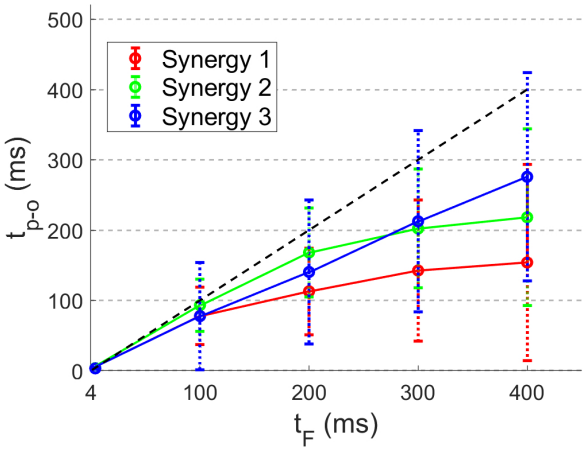

Fig. 6: Temporal anticipation according to forecast time.

VII. CONCLUSIONS

We propose a scheme for predicting STS motion using a DNN and considering muscle synergy. Our experimental results show that the temporal prediction of muscle synergy reaches high accuracy with a certain anticipation time of actual motion. Specifically, the prediction of synergy 2 leads to an anticipation time of over 200 ms which is longer than the time required for a typical pneumatic device to deliver its full strength. The accuracy of predicted values is approximately 90% for a 300 ms forecast time. We expect that STS motion prediction can provide valuable information on the power assistance required throughout motion. The timely control of actual assistive devices is likely feasible because STS motion intention can be properly predicted using the proposed scheme.

Various challenges remain to be addressed. For instance, the stability of the anticipation time was estimated experimentally (Fig. 6). However, further experiments are necessary to confirm that the anticipation time remains stable over STS motions performed under different conditions. Similar experiments are also necessary for confirming the accuracy of the scheme regarding muscle synergy activation. Those evaluations should also be performed when operating actual assistive devices to adapt to activities of daily living that require power assistance.

REFERENCES

[1] J.-i. Furukawa, S. Okajima, Q. An, Y. Nakamura, and J. Morimoto, "Selective assist strategy by using lightweight carbon frame exoskeleton robot," *IEEE Robotics and Automation Letters*, vol. 7, no. 2, pp. 3890–3897, 2022.

[2] Y. Kuroda, Q. An, H. Yamakawa, S. Shimoda, J.-i. Furukawa, J. Morimoto, Y. Nakamura, and R. Kurazume, "Development of a chair to support human standing motion -seat movement mechanism using zip chain actuator-," in *2022 IEEE/SICE International Symposium on System Integration (SII)*, 2022, pp. 555–560.

[3] T. Ito, J.-i. Furukawa, Q. An, J. Morimoto, and Y. Nakamura, "Muscle synergy analysis under fast sit-to-stand assist: A preliminary study," in *Proceedings of the Augmented Humans International Conference 2023*. New York, NY, USA: Association for Computing Machinery, 2023, p. 320–322.

[4] S. Neťuková, O. Klempíř, R. Krupička, P. Dušek, P. Kutílek, Z. Szabó, and E. Růžička, "The timed up & go test sit-to-stand transition: Which signals measured by inertial sensors are a viable route for continuous analysis?" *Gait & Posture*, vol. 84, pp. 8–10, 2021.

[5] M. Wairagkar, E. Villeneuve, R. King, B. Janko, M. Burnett, V. Agarwal, D. Kunkel, A. Ashburn, R. S. Sherratt, W. Holderbaum, and W. S. Harwin, "A novel approach for modelling and classifying sit-to-stand kinematics using inertial sensors," *PLOS ONE*, vol. 17, no. 10, pp. 1–25, 10 2022.

[6] H. Wang, S. Xu, J. Fu, X. Xu, Z. Wang, and R. S. Na, "Sit-to-stand (sts) movement analysis of the center of gravity for human–robot interaction," *Frontiers in Neurorobotics*, vol. 16, 2022.

[7] P. R. Cavanagh and P. V. Komi, "Electromechanical delay in human skeletal muscle under concentric and eccentric contractions," *European Journal of Applied Physiology and Occupational Physiology*, vol. 42, pp. 159–163, 1979.

[8] N. Yang, Q. An, H. Yamakawa, Y. Tamura, A. Yamashita, and H. Asama, "Muscle synergy structure using different strategies in human standing-up motion," *Advanced Robotics*, vol. 31, no. 1-2, pp. 40–54, 2017.

[9] S. Stroeve, "Learning combined feedback and feedforward control of a musculoskeletal system," *Biological Cybernetics*, vol. 75, pp. 73–83, july 1996.

[10] S. Muceli, A. T. Boye, A. d'Avella, and D. Farina, "Identifying representative synergy matrices for describing muscular activation patterns during multidirectional reaching in the horizontal plane," *Journal of Neurophysiology*, vol. 103, no. 3, pp. 1532–1542, 2010.

[11] A. S. Oliveira, L. Gizzi, D. Farina, and U. G. Kersting, "Motor modules of human locomotion: influence of emg averaging, concatenation, and number of step cycles," *Frontiers in Human Neuroscience*, vol. 8, 2014.

[12] J. Ilham, Y. Nakamura, T. Ito, K. Kondo, Q. An, J. Akita, and M. Toda, "Improving repeatability of surface electromyography measurement of sit-to-stand motions by using muscle synergy," *Biomedical Signal Processing and Control*, vol. 93, p. 106185, 2024.

[13] C. A. Doorenbosch, J. Harlaar, M. E. Roebroeck, and G. J. Lankhorst, "Two strategies of transferring from sit-to-stand; the activation of monoarticular and biarticular muscles," *Journal of Biomechanics*, vol. 27, no. 11, pp. 1299–1307, 1994.

[14] M. Hughes, D. Weiner, M. Schenkman, R. Long, and S. Studenski, "Chair rise strategies in the elderly," *Clinical Biomechanics*, vol. 9, no. 3, pp. 187–192, 1994.

[15] E. Papa and A. Cappozzo, "Sit-to-stand motor strategies investigated in able-bodied young and elderly subjects," *Journal of Biomechanics*, vol. 33, no. 9, pp. 1113–1122, 2000.

[16] H. J. Hermens, B. Freriks, C. Disselhorst-Klug, and G. Rau, "Development of recommendations for semg sensors and sensor placement procedures," *Journal of Electromyography and Kinesiology*, vol. 10, no. 5, pp. 361–374, 2000.

[17] M. Roebroeck, C. Doorenbosch, J. Harlaar, R. Jacobs, and G. Lankhorst, "Biomechanics and muscular activity during sit-to-stand transfer," *Clinical Biomechanics*, vol. 9, no. 4, pp. 235–244, 1994.

[18] F. Hug, N. A. Turpin, S. Dorel, and A. Guével, "Smoothing of electromyographic signals can influence the number of extracted muscle synergies," *Clinical Neurophysiology*, vol. 123, no. 9, pp. 1895–1896, 2012.

[19] P. Kieliba, P. Tropea, E. Pirondini, M. Coscia, S. Micera, and F. Artoni, "How are muscle synergies affected by electromyography preprocessing?" *IEEE Transactions on Neural Systems and Rehabilitation Engineering*, vol. 26, no. 4, pp. 882–893, 2018.